X CONGRESSO NACIONAL DE ENGENHARIA MECÂNICA 2018
20 A 24 DE MAIO DE 2018 SALVADOR – BA – BRASIL

DESIGN AND KINEMATIC ANALYSIS OF THE LINEAR DELTA ROBOT WITH SINGLE LEGS FOR ADDITIVE MANUFACTURING

Efrain Rodriguez, efrain.rodriguez@aluno.unb.br[1]
Cristhian Riaño, cristhian.riano@unipamplona.edu.co[1]
Alberto Alvares, alvares@alvarestech.com[1]

[1]Department of Mechanical and Mechatronics Engineering, University of Brasilia, GIAI (Grupo de Inovação em Automação Industrial), 70910-900, Campus Universitário Darcy Ribeiro, Asa Norte, PO Box: 04386, Brasilia, Brazil

Abstract: *This article deals with the design and kinematic analysis of a new structure of the linear delta robot using single legs for Additive Manufacturing (AM)/3D printing. The design is approached through a structured methodology based on a reference model for the of mechatronic product development, which consists of three design domains: mechanical, electro-electronic and computational. A new structure for the linear delta robot is proposed using an innovative concept of delta mechanism with single legs and rotational joints. The new structure consists of twelve links (three parallel single legs), three prismatic joints and eleven rotational joints.The inverse and direct kinematic problems are solved for the proposed structure. Finally, a prototype of the robot is developed to validate the design concepts and functionality of the machine.*
Keywords: *linear delta robot, single legs, parallel kinematic, additive manufacturing, 3D printing*

1. INTRODUCTION

Additive Manufacturing (AM), also referred as 3D Printing or Rapid Prototyping, brings together a set of technologies that allow the fabrication of physical objects by adding successive layers of material from a CAD model, in contrast to subtractive manufacturing processes. Since its inception in the 1980s, AM has experienced a considerable progress and expansion. More than 870 machines and 1500 materials of AM are now available in the market (Senvol LLC, 2018). Its wide expansion covers areas of engineering such as aeronautics and automotive, architecture, biomedical, product development, etc. due to its unique capabilities to reduce time-to-market, facilitate the fabrication of objects with complex geometries, enable mass customization, reduce the supply chain, and so on. (Huang *et al.*, 2015).

According to ISO/ASTM 52900 (ISO/ASTM 52900, 2015), AM processes are classified into seven categories depending on the type of material (solid, liquid and powder) and the manufacturing technique used. Thus, AM can be made by: binder jetting, directed energy deposition, material extrusion, material jetting, powder bed fusion, sheet lamination and vat photopolymerization. This wide variety of technologies has allowed AM not to be reserved only for the prototyping of parts, but now also for the production of functional parts with high added value. Within the material extrusion manufacturing category, the Fused Deposition Modeling (FDM) technique, introduced by Stratasys in 1989 (Crump and Stratasys, 1989), is one of the most popular and used for its simplicit and low cost, becoming attractive to small and medium enterprises. As shown in Figure 1, this process consists of pushing a filament into an extruder by means of a stepper motor coupled with a gear system, allowing its extrusion through the spout having a smaller diameter than the filament. The extruded filament is deposited on the top of the platform or above the anterior layer.

Many efforts have focused on the improvement of FDM performance in different fields, such as materials Singh *et al.* (2017), process parameters optimization Mohamed *et al.* (2015), and sustainability Kondoh *et al.* (2017). However, even though some studies have highlighted that the optimization of the architecture and kinematics of FDM machines are key issues in order to improve AM quality and reduce build time Allen and Trask (2015); Song *et al.* (2015), this subject has not been given the deserved attention. With this in mind, some researchers have considered the design of FDM machines with parallel kinematics Allen and Trask (2015); Fiore *et al.* (2015); Song *et al.* (2015); Ye *et al.* (2017).

In this context, this research presents the design and kinematic analysis of a new linear delta robot structure with single legs and rotational joints for AM using FDM process. In section 2.design methodology based on a reference model for mechatronics products development is presented. Section 3deals with the mechanical design presenting the kinematic analysis and mechanical subsystems description. Section 4outlines the electro-electronic design and section 5presents the computational design. Finally, section 6presents the main conclusions of this work.

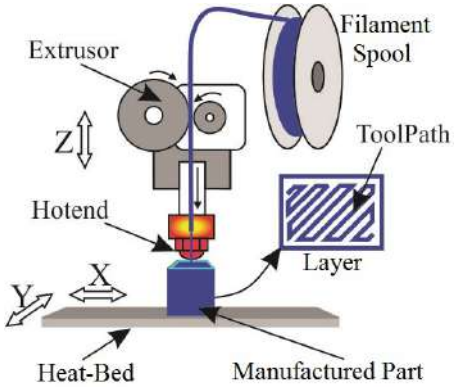

Figura 1: FDM process representation.

2. DESIGNMETHODOLOGY

Since September 2000, the German Association of Engineers and Professor Gausmeier has been working on the development of a new reference model, called the V model under the industrial guide VDI 2206 (Gausemeier and Moehringer, 2003). The model presented in Fig. 2 aims to provide a structured methodology to support the design of mechatronic systems in a systematic way. Such methodology can be understood as a specific reference model for the development of mechatronic products. This model proposes a flexible procedure that can be adapted to a specific product. In addition, it is not intended to replace existing models, but aims to complement the models focused on an individual domain (mechanical, electronic or computational), even if the generic character models.

From a macro perspective, the starting point of model V is the definition of a design task for an individual mechatronic product. Therefore, a set of product requirements are established for the project task being executed, which will represent a reference target for the validation of the future product. An extended description of this model can be found in (Gausemeier and Moehringer, 2003). In this work, V model is used in the process of development of the Linear Delta robot of AM (referred in this paper as rDL-AM) to describe each of the mechanical, electro-electronics and computational domains.

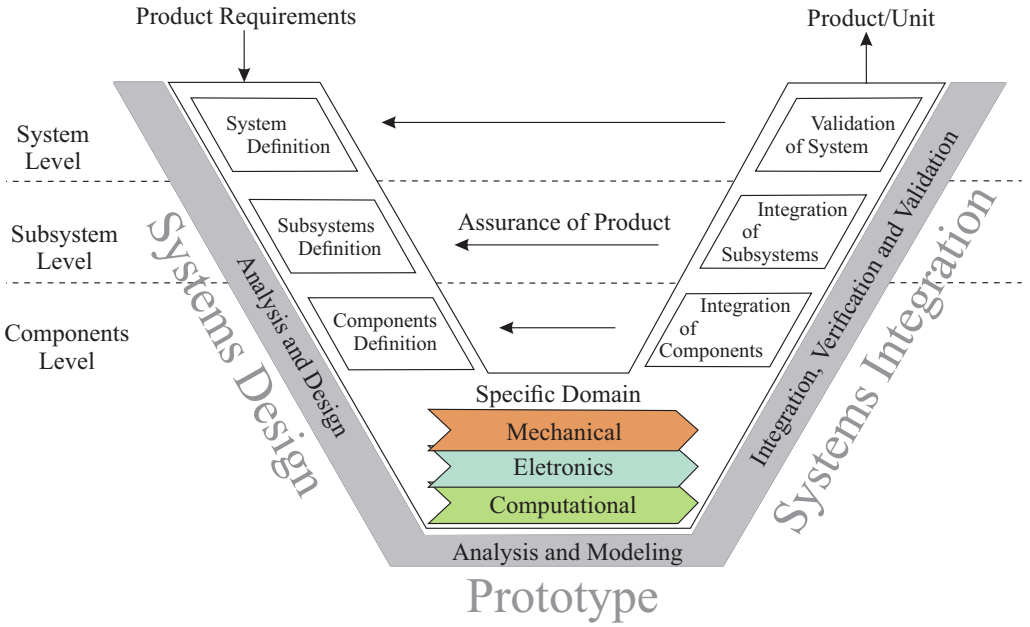

Figura 2: VDI model for development of mechatronic products (Vasić and Lazarević, 2008).

.

3. MECHANICAL DESIGN

3.1 Inverse Kinematics

The problem of computing the possible actuated joints coordinates of a robot given the end-effector pose is called inverse kinematic problem. The resolution of this problem is essential for position control of the Linear Delta robot for FDM. The kinematic model and geometric parameters of the Linear Delta robot are shown in Fig. 3, where the reference coordinate system O is located on the printing platform on the center of the fixed base A-B-C, with the z-axis normal to the

printing platform and the *x*-axis in the *A* direction. The actuated prismatic joints are denoted by $Q_i(x_i, y_i, z_i)$, with *i=1, 2, 3,* which are located at a distance R_b from the reference system *O* and spaced 120° apart from each other (see the top view in Fig. 3). The common-joint pose respect to the reference system is denoted by *P(x, y, z)*. The aim is to determine the (x_i, y_i, z_i) coordinates for the actuated joints.

From Fig. 3, the expressions in Eq. (1) can be deduced to obtain the (x_i, y_i) coordinates of each actuated joints Q_i.

$$x_i = R_b\, cos\theta_i, \quad y_i = R_b\, sin\theta_i, \quad i = 1, 2, 3, \tag{1}$$

where

$$\theta_i = \frac{2i-2}{3}\pi, \quad i = 1, 2, 3, \tag{2}$$

It is assumed that all the three legs of the Linear Delta robot are identical in length (L_e). The (x_i, y_i) coordinates are used to compute z_i by using Pythagoras through the Eq. (3).

$$z_i = z \pm \sqrt{L_e^2 - (x - x_i)^2 - (y - y_i)^2}, \quad i = 1, 2, 3, \tag{3}$$

In Eq. (1), the notation $\pm$ means that there are two possible solutions for the Linear Delta robot pose. However, in this work only the solution with sign + that results in the configuration of the robot shown in Fig. 3 is considered, thus completing the procedure for the inverse kinematics of the Linear Delta robot.

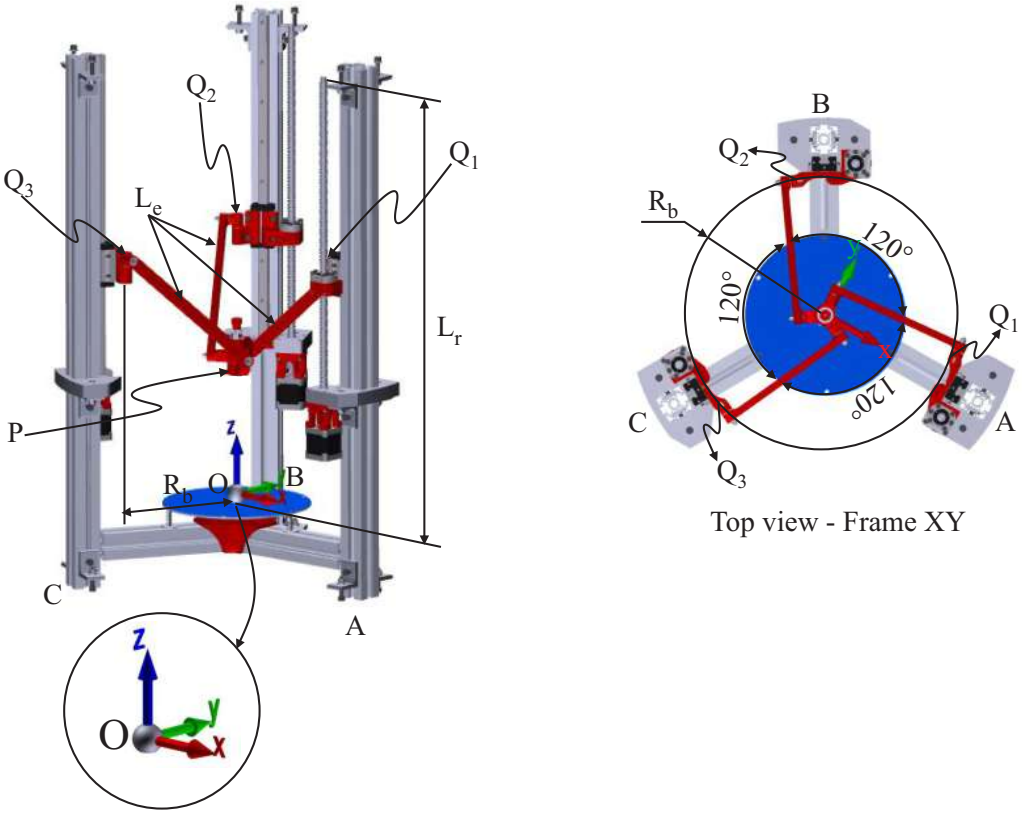

Figura 3: A kinematics model of the Linear Delta robot

3.1.1 Forward Kinematics

In contrast with inverse kinematics, the forward kinematics problem is to find the pose of the end-effector relative to the base given the actuated joints coordinates. Solving the linear delta's forward kinematics problem is not as trivial as in inverse kinematics problem since the procedures for finding a solution involves more mathematical complexity.

The forward kinematics model of the Linear Delta robot can be represented as the intersection of three spheres as illustrated in Fig. 4(a). The centers of the three spheres are given by the prismatic joints points $Q_i(x_i, y_i, z_i)$ (with *i*=1, 2, 3) and the radius of each sphere is equivalent to the length of the corresponding leg. The solution(s) for the Linear Delta robot end-effector pose can be obtained from the point(s) of intersection between the three spheres. Obtaining the solution(s) is subject to three possible situations: (1) when a sphere is a tangent to the intersection of the other spheres,

resulting in a unique solution; (2) when there are two points of intersection between the spheres resulting in two possible solutions; and, (3) when there is no intersection between the spheres resulting in an unsolvable system.

A fourth situation could arise when the centers of two or more spheres coincide with the same point, and the system has infinite solutions. However, in the case of the Linear Delta robot, this situation is impossible. The relationship between the coordinates of each actuated prismatic joint and the coordinates of the common-joint of the Linear Delta robot can be described by expression in Eq. (4), which represents the equation of the sphere corresponding to each kinematic chain of the robot.

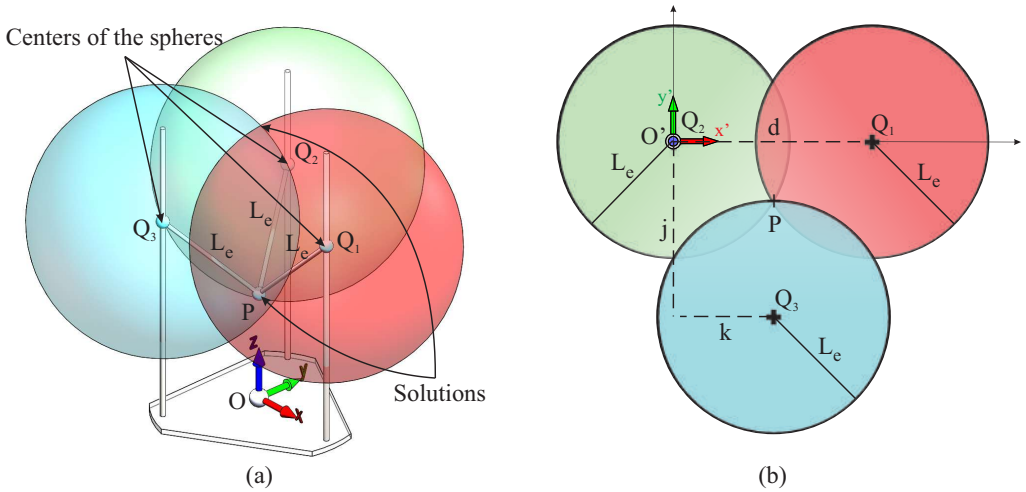

Figura 4: Forward kinematics problem: (a) the Linear Delta robot represented as the intersection of three spheres. (b) Translation of the coordinate reference system based on the Trilateration concept

.

$$(x - x_i)^2 + (y - y_i)^2 + (z - z_i)^2 = L_e^2, \quad i = 1, 2, 3, \tag{4}$$

In order to find the point(s) of intersection between the three spheres, the Trilateration method has been used which allows for the determination of the absolute or relative locations of the points by the measurement of distances, using the geometry of circles, spheres or triangles. To compute the intersection of three spheres by using the Trilateration method we must consider that

- all three centers are in the plane $z = 0$,
- one sphere center is at the origin, and
- one other is on the x-axis.

Following this approach, the coordinate system of reference O, now denoted by O', has been moved to one center sphere Q_2 as shown in Fig. 4(b). Therefore, the equations of the spheres respect to the new reference system can be rewritten as:

$$\begin{aligned} L_e^2 &= x'^2 + y'^2 + z'^2 \\ L_e^2 &= (x' - d)^2 + y'^2 + z'^2 \\ L_e^2 &= (x' - k)^2 + (y' - j)^2 + z'^2 \end{aligned} \tag{5}$$

The equation set that allow computing the unknowns x', y' and z' can be obtained by reducing the system in Eq. (5). Then we have:

$$x' = \frac{1}{2}d \tag{6}$$

$$y' = \frac{k^2 + j^2}{2j} - \frac{k}{j}x \tag{7}$$

$$z' = \pm\sqrt{L_e^2 - x^2 - y^2} \tag{8}$$

where *k* is the signed magnitude of the *x* component of the vector from Q_2 to Q_3, *d* is the distance between the centers Q_2 and Q_1 and *j* is the signed magnitude of the *y* component of the vector from Q_2 to Q_3. This values can be computed from Eq. (9), Eq. (10) and Eq. (11).

$$k = \hat{e}_x \cdot (Q_3 - Q_2) \tag{9}$$

$$d = ||Q_1 - Q_2|| \tag{10}$$

$$j = \hat{e}_y \cdot (Q_3 - Q_2) \tag{11}$$

Q_1, Q_2, and Q_3 are treated as vectors in the original coordinate system *O*. Similarly, $\hat{e}_x$ and $\hat{e}_y$ are unit vectors, the first in the direction Q_2 to Q_1 and the second in the *y*-direction, both in the original coordinate system. These unit vectors can be calculated through Eq. (12) and Eq. (13) respectively.

$$\hat{e}_x = \frac{Q_1 - Q_2}{||Q_1 - Q_2||} \tag{12}$$

$$\hat{e}_y = \frac{Q_3 - Q_2 - k\hat{e}_x}{||Q_3 - Q_2 - i\hat{e}_x||} \tag{13}$$

The third unit vector can be obtained by using the cross product properties as $\hat{e}_z = \hat{e}_x \times \hat{e}_y$.

With this, the system solution(s) represented by the intersection of the three spheres, with respect to the original coordinate system, can be obtained from Eq. (14).

$$\vec{p}_{1,2} = Q_2 + x\hat{e}_x + y\hat{e}_y \pm z\hat{e}_z \tag{14}$$

Usually, the intersection of the three spheres results in two solution points which, in this case, describe two possible positions of the end-effector respect to the base. For this reason, the notation $\pm$ appears in Eq. (14). In this work, we opt for the solution with sign + that describes the configuration of the robot shown in Fig. 4(a).

3.1.2 Differential Relations

The differential relations model determines the relationship between velocities of the end-effector and the velocities of the actuated joints. Both vectors of velocities can be obtained through the Jacobian matrix. The Linear Delta robot differential relations model is obtained by differentiating Eq. (3) with respect to time and rearranging them as follow:

$$\dot{q} = J\dot{p} \tag{15}$$

where $\dot{q}$ is the vector of actuated joint velocities, *J* the Jacobian matrix, and $\dot{p}$ the vector of end-effector velocities. Them, the Eq. (15) can be written as:

$$\begin{bmatrix} \dot{z_1} \\ \dot{z_2} \\ \dot{z_3} \end{bmatrix} = \begin{bmatrix} \frac{x-x_1}{z-z_1} & \frac{y-y_1}{z-z_1} & 1 \\ \frac{x-x_2}{z-z_2} & \frac{y-y_2}{z-z_2} & 1 \\ \frac{x-x_3}{z-z_3} & \frac{y-y_3}{z-z_3} & 1 \end{bmatrix} \begin{bmatrix} \dot{x} \\ \dot{y} \\ \dot{z} \end{bmatrix} \tag{16}$$

3.2 Subsystems description

3.2.1 Base structure of the rDL-AM

The detailing base structure of the rDL-AM is shown in Fig. 5. It formed basically by plates and aluminum profiles. The two main plates (bottom and top) are attached to three parallel aluminum profile columns. Three smaller plates, referred as central brackets, are fixed to the aluminum profiles at a distance of 500 mm measured from the top-plate. The aluminum plates have a dimensions of 500 mm x 500 mm and thickness of 20 mm, while the profiles are 40 mm x 40 mm x 1000 mm. Figure 5 also shows a detail of the central brackets fixation on the aluminum profiles using aluminum corner brackets, the same one used to fix the main plates. The goal of a structure based on aluminum plates and profiles is to achieve the greatest possible robustness and rigidity. For aluminum plates, adjustment tolerances have been defined for the geometries that are in contact with the aluminum profiles in order to generate fixation interferences in the assembly process. Thus, adjustment tolerances have been defined for the cavities where the profiles and bearings are inserted. Furthermore, Fig. 5 also presents a detail of the substructure corresponding to the printing base, which consists of three short profiles that hold the heat-bed fixed to the main frame near the bottom plate.

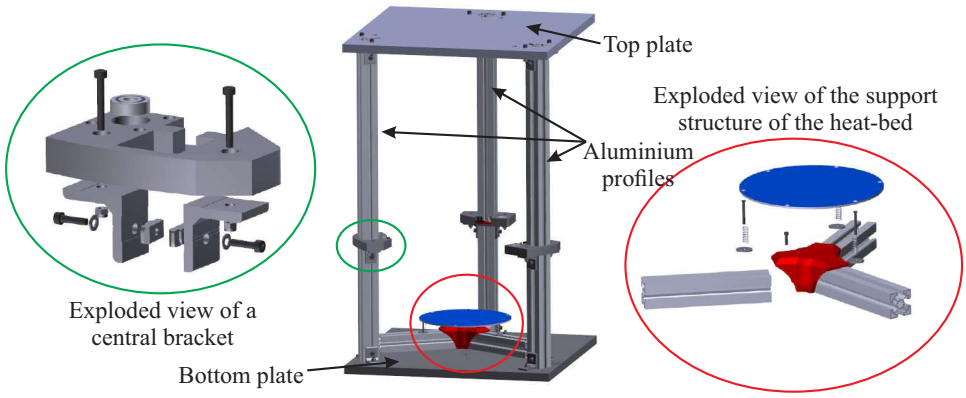

Figura 5: Structure.

3.3 Delta mechanism description

Figure 6 presents the delta mechanism designed for the rDL-AM, which has as a differential feature the use of single legs and rotational joints. This feature was conceived by the designing team in a stage of design principles formulation and selection. Each leg is formed of three links: the primary link, which connects the delta mechanism to the motion transmission system; the main arm, which transmits the movement generated by the linear actuators to the end-effector (hotend); and, the secondary link, that constitutes the mechanism common-joint where the hotend is coupled.

The three primary links are identical in geometry and dimensions, just like the arms, but the three secondary links have different shapes. The rotational joints that allow mobile between the links are based on 624-RS ball bearings inserted in the arms. The fixing is made by screws. In the common-joint, a drilled shaft is used to fix the secondary links allowing mobility through bearings 608-RS and, in turn, functions as a guide for the filament.

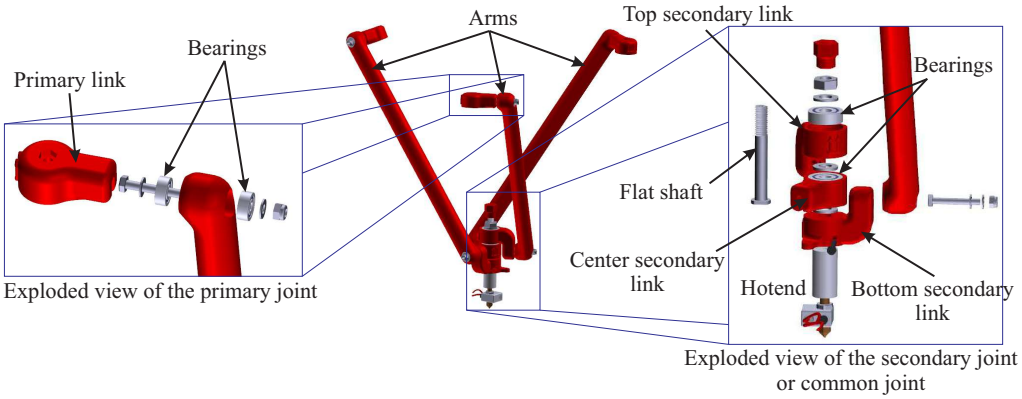

Figura 6: The delta mechanism with single legs and rotational joints.

3.4 Extruder mechanism description

The extruder mechanism adopted in this project is bowden type. That is, the extruder body is fixed in the base structure of the robot, while only the hotend is assumed as end-effector. Thus, the plastic filament is pushed by the extruder and guided through a teflon tube/hose to the hotend. This type of extruder allows to remove weight from the robot mechanism, since extruder body weight is supported on the base structure.

The extruder designed for the rDL-AM is shown in Fig. 7. This consists of a main body with a mechanism that presses the filament against the toothed pulley that pushes it. The pressure is exerted by a spring incorporated in the mechanism. The torque to push the filament is provided by a NEMA stepper motor 17 coupled to the extruder body. The shape design of this extruder is original, which facilitates placement of the filament by the user through the push-button mechanism concept.

It is necessary to define a mathematical expression to calculate the motor steps per millimeter unit of extruded filament. This expression is given by:

$$P_u = \frac{P_m F}{d\pi} \tag{17}$$

where,

- P_u is: steps per millimeter unit of filament to be extruded;

- P_m is: steps per revolution of the motor (typically 200 steps for NEMA 17);
- F is: micro-step factor (2, 4, 8 or 16); and,
- d is: pulley effective diameter.

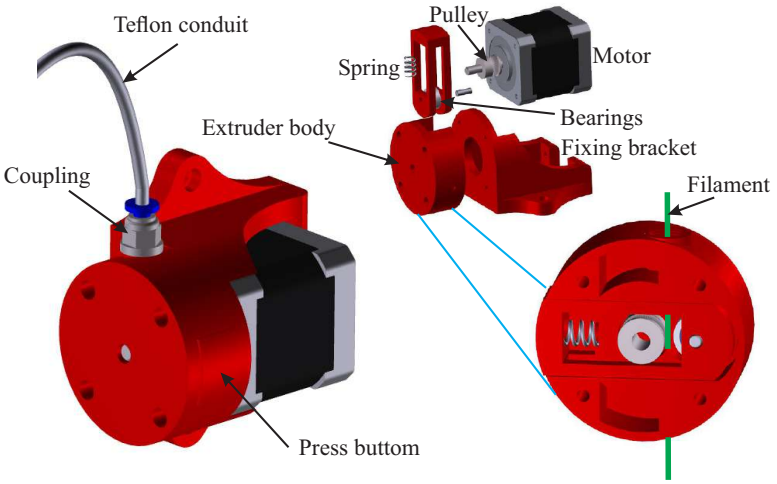

Figura 7: Detailing the extruder mechanism

3.5 Motion transmission system

In order to satisfy the precision requirement of the robot, recirculating ball screw-nut and linear guide rail-slide systems were selected as solution principles for the motion transmission system, which is shown in Fig. 8. The torque input is provided by a NEMA 17 stepper motor coupled with the ball screw (5mm thread pitch) through a flexible coupling (5mm x 8mm). The recirculating ball nut is attached to the slide-car using a screwed printed plastic part. The rail (15 mm)-slide system has the function of maintaining the linearity of the movement. The bearings support the ball screw between the central and top aluminum plates.

The expression that allows to calculate the motor steps to generate a movement of one millimeter on the linear actuator, is given by:

$$P_u = \frac{P_m F}{n} \tag{18}$$

where,

- P_u is: steps per millimeter unit of motion;
- P_m is: steps per revolution of the motor (typically 200 steps for NEMA 17);
- F is: micro-step factor (2, 4, 8 or 16); and,
- d is: thread pitch on the ball screw.

4. ELECTRO-ELECTRONICS DESIGN

The simplified diagram of the rDL-AM electro-electronic system is shown in Fig. 9. This system uses a controller based on Arduino technology, specifically the reference board Arduino Mega 2560. The advantages of using the Arduino include an open technology, low cost, easy to use and has compatibility with lots of electronic modules for different applications. Additionally, the technological extension shield RAMPS 1.4 is coupled with the Arduino in order to facilitate the external devices connection such as sensors, actuators, etc.

The drivers used to control the stepper motors are commercial reference A4988, which have connection compatibility with the Ramps 1.4 board. The A4988 allows two-way direction control, limit current adjustment and micro-step split with five resolutions up to 1/16 of the motor step. In addition, they have an operating capacity of 8-35 V and a current 2 A maximum. In total four drivers are used for the rDL-AM, one for each X, Y and Z axis motor and one for the extruder motor.

The rDL-AM uses four stepper motors in total, one for each machine axis and one for the extruder mechanism. The X-Y-Z axis motor current was set at 200 mA and 400 mA for the extruder motor.

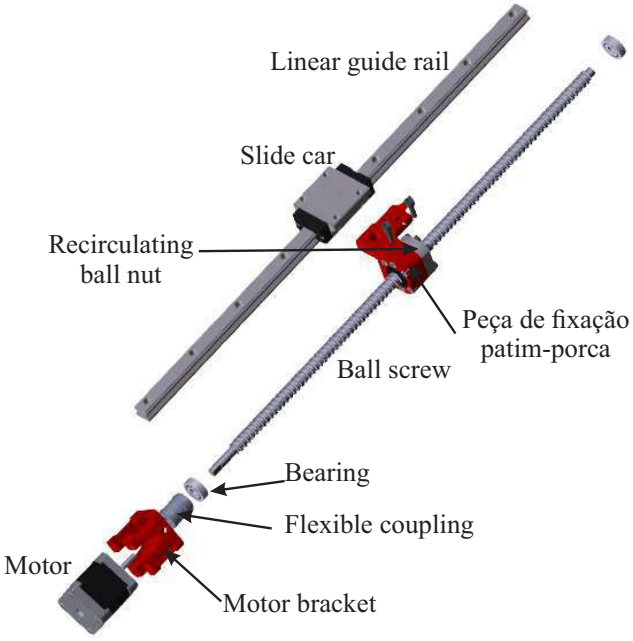

Figura 8: Motion transmission system

Optical endstop sensors are used for end-of-course protection and homing movements. The rDL-AM uses two optical sensors per axis. Also, thermistors are used for the temperature control both of the heatbed and the extruder.

The E3D hotend model has a 12 V resistor and a 0.3 mm resolution nozzle. A fan is built into hotend to cool it down and prevent clogging of material. A heated bed with 200 mm diameter and a 12 V resistance is used.

Finally, the switched power supply capable of working at voltages 110-220 V, delivering a 12 V voltage and 20 A current on the output.

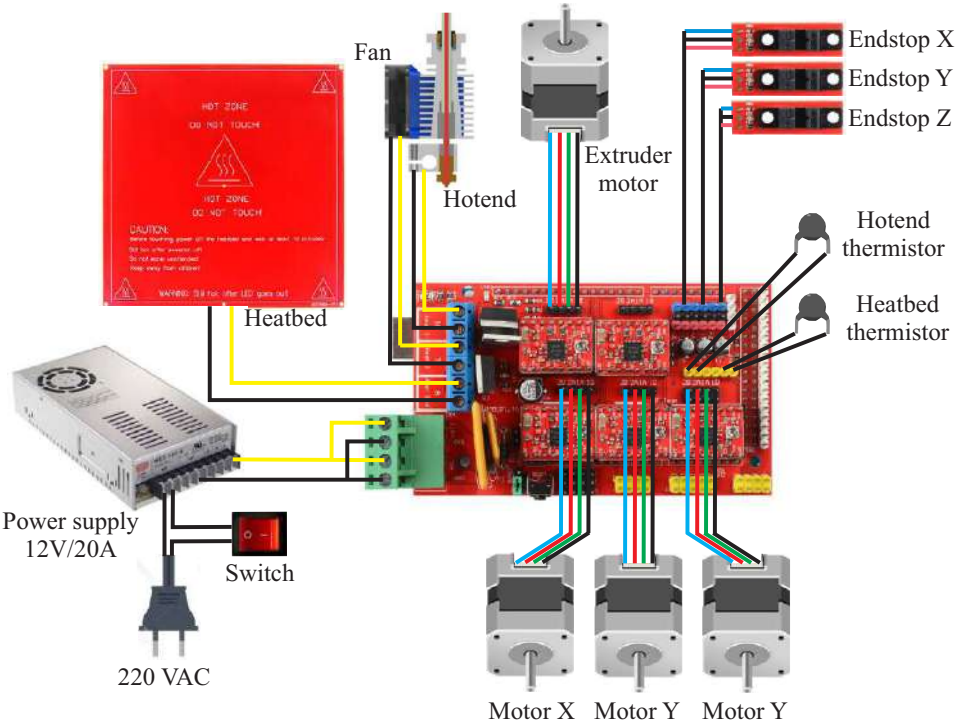

Figura 9: Electro-electronics system schematic

5. COMPUTATIONAL DESIGN

The software modules used to control the rDL-AM are based on open-source software programs. In general, the rDL-AM computational system consists of three primary modules: firmware, slicing software and control interface. The general description scheme of the rDL-AM computational system is presented in Fig. 10.

The firmware is the program code mounted on the machine controller, which enables communication with the control

software. This work has been adequate and used the *Marlin* firmware, developed by the RepRap international project under open source license for 3D printers with Arduino technology controller. Marlin contains code functions for serial communication, interpretation of G-code instructions, temperature control, kinematic control, interrupt protection, and more. To implement the Marlin in the rDL-AM it was necessary to make some simple adjustments and configurations in the code, regarding the inclusion of the model and kinematic parameters of rDL-AM and the number of steps per millimeter of the transmission and extruder systems. The steps per millimeter for the extruder motor were calculated through the Eq. 17, obtaining the value of 84.90 steps per millimeter, and for the transmission system through Eq.18, resulting in 640 steps per millimeter. Moreover, some settings were made for endstops, maximum working speed and acceleration, homing speed, etc.

As control interface software was used *Repetier Host*, which is a computational environment that allows to establish communication with the machine/3D printer, adapt the workspace shape, upload a part 3D model, make automatic and manual control and monitor the printing process. Repetier Host integrates slicer software into its computing suite. The slicing software for printing program generation integrated into the Repetier Host usually are *Slic3r, CuraEngine* and *SKeinforge*. All have advantages and disadvantages, but in this project it was preferred to use Slic3r as software for generating the G-code program. Slic3r allows setting process parameters, material and printer parameters.

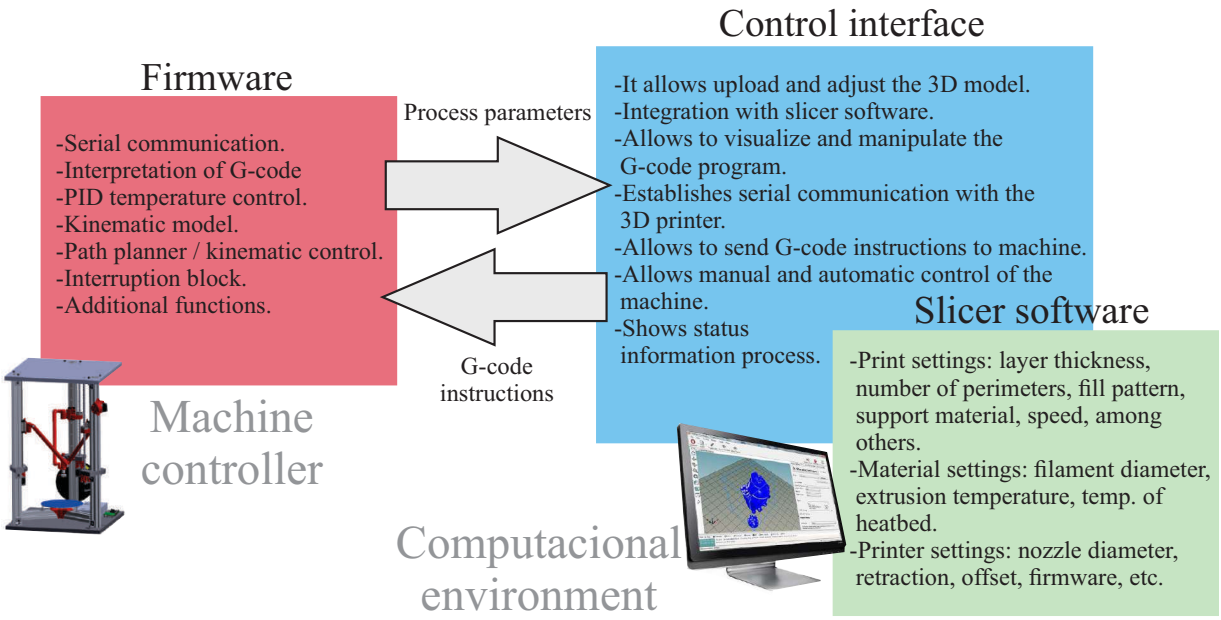

Figura 10: Computational system of the rDL-AM

6. CONCLUSIONS

In this work, the design and kinematic analysis of a robot with linear delta parallel kinematics for additive manufacturing was presented. The rDL-AM has as main differential the use of an innovative concept of delta mechanism with single legs and rotational joints. This solution is also different from the conventional delta architectures that have a mobile platform, while the rDL-AM has a common joint where the end-effector is directly coupled. The inverse and direct kinematic problems of the robot were solved. The approach based on the concept of Trilateration allowed solving the direct kinematic problem of the proposed delta mechanism. The adoption of a specific reference model for mechatronic product development served as a guideline to systematize the design activities involved in each of the domains ones that make up the robot (mechanical, electro-electronic and computational). In order to validate the design feasibility of the proposed Linear Delta robot for AM, a prototype of the machine has been developed. Fig. 11 shows such a prototype of the rDL-AM with aluminum base structure achieved after the validation of the first prototype with wooden base structure presented in a previous work (Rodriguez *et al.*, 2017). The URL (https://tinyurl.com/y734fwes) presents a prototype video of the delta linear machine in operation: printing of a part with complex geometry.

In future works, the aim is to study the robot's kinematic reconfiguration and perform uncertainty and clearances analysis of links and joints. Also, there is the idea to use the robot as a platform for the implementation of a controller based on the new STEP-NC numerical control standard.

7. ACKNOWLEDGMENTS

CNPq, DPG/UnB.

Figura 11: Prototype of the Linear Delta robot for AM.

8. REFERÊNCIAS

Allen, R.J.A. and Trask, R.S., 2015. "An experimental demonstration of effective Curved Layer Fused Filament Fabrication utilising a parallel deposition robot". *Additive Manufacturing*, Vol. 8, pp. 78–87. ISSN 22148604. doi: 10.1016/j.addma.2015.09.001.

Crump, S.S. and Stratasys, I., 1989. *Apparatus and method for creating three-dimensional objects*.

Fiore, E., Sbaglia, L. and Milano, P., 2015. "Dimensional Synthesis of a 5-DOF Parallel kinematic Manipulator for a 3D printer". In *16th International Conference on Research and Education in Mechatronics*. IEEE, pp. 41–48. doi: 10.1109/REM.2015.7380372.

Gausemeier, J. and Moehringer, S., 2003. "New Guideline VDI 2206 – A Flexible Procedure Model for Specific Requirements to the Design of Mechatronic Systems". *International Conference on Engineering Design Iced 03 Stockholm*, p. 10. ISSN 22204342.

Huang, Y., Leu, M.C., Mazumder, J. and Donmez, A., 2015. "Additive manufacturing: current state, future potential, gaps and needs, and recommendations". *Journal of Manufacturing Science and Engineering*, Vol. 137, No. 1, p. 14001. doi:10.1115/1.4028725.

ISO/ASTM 52900, 2015. "Additive manufacturing — General principles — Terminology".

Kondoh, S., Tateno, T., Kishita, Y., Komoto, H. and Fukushige, S., 2017. "The potential of additive manufacturing technology for realizing a sustainable society". In M. Matsumoto, K. Masui, S. Fukushige and S. Kondoh, eds., *Sustainability Through Innovation in Product Life Cycle Design*, Springer Singapore, EcoProduction, pp. 475–486. ISBN 978-981-10-0469-8 978-981-10-0471-1. doi:10.1007/978-981-10-0471-1_32.

Mohamed, O.A., Masood, S.H. and Bhowmik, J.L., 2015. "Optimization of fused deposition modeling process parameters: a review of current research and future prospects". *Advances in Manufacturing*, Vol. 3, No. 1, pp. 42–53. ISSN 2095-3127, 2195-3597. doi:10.1007/s40436-014-0097-7.

Rodriguez, E., Riaño Jaimes, C. and Álvares, A.J., 2017. "Projeto mecatrônico de um robô com cinemática paralela delta linear para manufatura aditiva". In *Proceedings of the IX Congresso Brasileiro de Engenharia de Fabricação (COBEF)*. ABCM, pp. 1–10. doi:10.26678/ABCM.COBEF2017.COF2017-0282.

Senvol LLC, 2018. "Senvol database". URL `http://senvol.com/database/`.

Singh, S., Ramakrishna, S. and Singh, R., 2017. "Material issues in additive manufacturing: A review". *Journal of Manufacturing Processes*, Vol. 25, pp. 185–200. ISSN 15266125. doi:10.1016/j.jmapro.2016.11.006.

Song, X., Pan, Y. and Chen, Y., 2015. "Development of a low-cost parallel kinematic machine for multidirectional additive manufacturing". *Journal of Manufacturing Science and Engineering*, Vol. 137, No. 2, p. 21005. doi: 10.1115/1.4028897.

Vasić, V.S. and Lazarević, M.P., 2008. "Standard Industrial Guideline for Mechatronic Product Design". *FME Transactions*, Vol. 36, pp. 103–108. ISSN 1451-2092.

Ye, W., Fang, Y. and Guo, S., 2017. "Design and analysis of a reconfigurable parallel mechanism for multidirectional additive manufacturing". *Mechanism and Machine Theory*, Vol. 112, pp. 307–326. ISSN 0094114X. doi: 10.1016/j.mechmachtheory.2016.02.011.

9. RESPONSIBILITY NOTICE

The authors are the only responsible for the printed material included in this paper.